JOURNAL OF AIRCRAFT
Vol. 47, No. 1, January–February 2010

Engineering Notes

Bistable Composite Flap for an Airfoil

S. Daynes,* S. J. Nall,† P. M. Weaver,‡ K. D. Potter,§
P. Margaris,¶ and P. H. Mellor**
University of Bristol,
Bristol, England BS8 1TR United Kingdom

DOI: 10.2514/1.45389

I. Introduction

STANDARD aerospace structures typically possess a fixed geometry and aerodynamic control is possible only by the articulation of substructures using pinned joints (e.g., ailerons) and/or substructures that also translate (e.g., flaps and slats). These design solutions can be successfully used to control aircraft but they can have significant deficiencies with regard to aerodynamic performance, mass penalties, and complexity. There have been a number of shape-adaptive airfoil demonstrators in recent years that have attempted to address these problems [1–7]. The Intelligent Responsive Composite Structures (IRCS) program at the University of Bristol was initiated to investigate the design of adaptive structures using bistable composites as a means of providing aerodynamic control [8–10]. The program develops adaptive airfoil systems in which there is integration between the actuator, aerodynamics, and bistable structure.

However, the existing technology readiness level of bistable composite flaps is still quite low [11,12]. Also, there has not yet been a demonstrator program that integrates bistable composites and an actuator solution into a workable proof-of-concept demonstrator. The present research is directed towards meeting these challenges. A full-scale rotor blade section with a span of 2.114 m and a chord of 0.68 m, fitted with a 1 m span flap is wind-tunnel tested up to a speed of 60 m/s, with the flap moving between two stable states, for various angles of attack. For simplicity of analysis the blade is approximated as a NACA 24016 section with a 20% chord trailing-edge flap (see Fig. 1).

The trailing-edge flap is designed to change between its stable geometries between hover and forward flight conditions for aerodynamic performance improvements. The flap is driven by an electromechanical actuator that is mounted inside the blade D-spar at the leading edge. The design presented herein is inherently simple, has a low parts count, is lightweight, is all electric, is very modular in its construction, and is also highly maintainable. Also, the system has limited control authority and is independent of the primary flight controls for safety reasons. When not deployed the flap integrates into the rotor blade section so as to not change the center of mass or aerodynamic profile of the blade cross section. When the flap is deployed, it provides a smooth, continuous change in camber at the trailing edge. This continuous variation in camber has the potential to improve aerodynamic effects such as the point of trailing-edge separation and localized pressure spikes. The inherent bistability of the flap also has the potential to make this design very energy-efficient, because the actuator is only required to do work when moving between stable positions, not to hold these positions continuously.

II. Bistable Flap Design

The bistable flap itself consists of 20 bistable prestressed buckled laminates arranged in two rows. The details of how these bistable plates were manufactured is given in [3]. Each plate has dimensions of 100 by 100 mm and is made from Hexcel 913 glass-fiber-reinforced plastic (GFRP) prepreg. The selected layup used is $[0/90/90/0]_T$ for each plate, with prestressing being applied in the 0 deg (chordwise) direction. For these plates, 1.1% prestrain in total is applied during manufacture to induce bistable behavior. The resultant geometries of a typical GFRP prestressed buckled laminate manufactured are shown in Fig. 2.

All of the rotor blade structure remote from this bistable flap region is unmodified and is assumed to be completely rigid during wind-tunnel testing. The upper and lower external skins of the flap are manufactured from the same GFRP prepreg but are not bistable and have the layup $[90/0/90]_T$. The bistable plates are attached at one of their ends to a spar situated at 85% chord on the rotor blade. There is, however, a requirement for a discontinuity in the skin at the trailing edge, because there is a corresponding relative change in displacement of the external skin between the upper and lower surfaces during transition between stable states. This complication is unavoidable due to the restrictive geometry a cambering airfoil presents. Because this design feature is unavoidable, a skin discontinuity at the trailing edge is aerodynamically (and structurally) the most desirable solution to the problem. Foam tape was placed between each of the plates at the trailing edge. The foam material makes the airfoil weathertight and minimizes friction between the plates. The low shear stiffness of foam does not restrict the plates from sliding over each other significantly and hence does not affect their ability to be bistable. Finally, a sliding clamp is placed on the trailing edge to achieve the desired trailing-edge geometry. The total mass of the 1 m span bistable flap and additional rear spar is approximately 0.8 kg.

III. Actuator Design and Integration

In addition to volume and mass restrictions, some of the actuator design requirements considered were force, displacement, dynamic response behavior, power supply restrictions, and duty cycle. The work done by the actuator to change the bistable flap between stable states needs to be large enough to cause snap-through of the bistable plates and to also do work against the in-service aerodynamic loads [13,14]. Finite element (FE) modeling of the electromechanical actuator topology showed that the force and displacement behavior of the actuator could be tailored to the required force–displacement profile of the bistable airfoil. Design iterations were then undertaken using FE analysis to reduce the mass of the actuator further while retaining efficient performance.

The actuator consists of a permanent magnet mover, excited by two C-shaped electromagnetic cores, which translates with one degree of freedom between two displacement limits (see Fig. 3a).

Presented as Paper 2103 at the 50th AIAA/ASME/ASCE/AHS/ASC Structures, Structural Dynamics, Palm Springs, CA, 4–7 May 2009; received 11 May 2009; revision received 8 October 2009; accepted for publication 8 October 2009.

*Ph.D. Student, Department of Aerospace Engineering, Queen's Building. Member AIAA.
†Research Associate, Department of Electrical and Electronic Engineering, Queen's Building.
‡Professor, Department of Aerospace Engineering, Queen's Building. Member AIAA.
§Reader, Department of Aerospace Engineering, Queen's Building.
¶Lecturer, Department of Aerospace Engineering, Queen's Building.
**Professor, Department of Electrical and Electronic Engineering, Queen's Building.

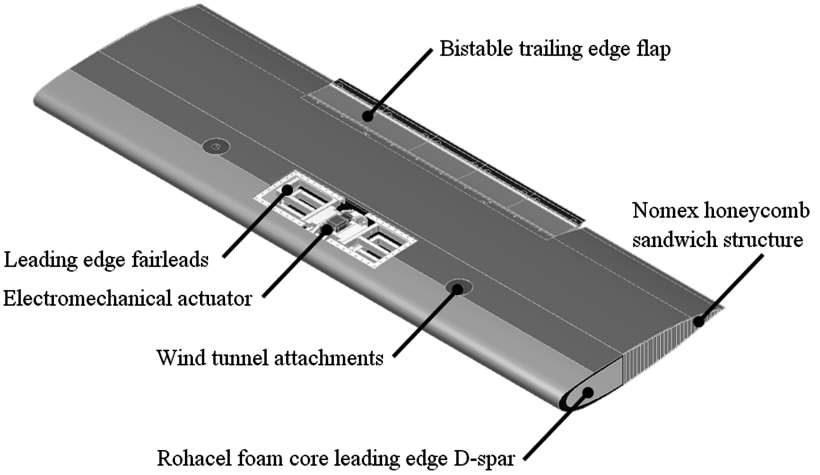

Fig. 1 Lower surface of IRCS bistable airfoil (actuator access panel removed).

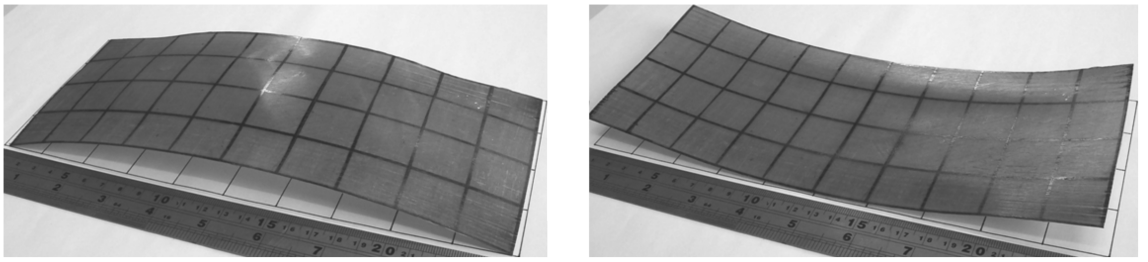

Fig. 2 Geometries of a typical GFRP bistable prestressed buckled laminate.

This topology is characterized by a high specific actuating force, accurately controlled displacements, and a relatively simple construction [15]. Figure 3b plots the measured force versus current characteristics of the device corresponding to the location of the mover. At the designed nominal 40 A current, an output force lying between 630 and 670 N was measured across the displacement range. The actuator has a specific work output of 6 J/kg based upon a total actuator mass of 3.5 kg.

The center of mass of the actuator was placed near the leading edge to coincide with the center of mass of the existing blade section. One key constraint was that production blade tooling could be used with only minor modifications. Using a standard rotor blade section, a chamber is created in the leading-edge D-spar to accommodate the actuator by cutting into the lower aerodynamic surface. A slot is cut out of the trailing-edge region to accommodate the bistable flap. Cord linkages are threaded through the blade before the trailing edge is attached. This modular design makes maintenance and inspection of the system possible. Actuator power supply cables are fed through the foam center of the D-spar back to the rotor hub.

The actuator was orientated so its operation is not affected by blade lagwise or flapwise in-service loading. These two dynamic loads are oscillatory in nature and their frequency is a function of rotor rotation frequency. Centrifugal loads will also affect the operation of the actuator. However, centrifugal loads are of relatively constant magnitude for a particular rotor angular speed, so they can be offset by changing the preload of the two cords if required. There is a screw thread at the end of each chord where they are attached to the actuator in the D-spar. These screw threads enable the cords to be preloaded. Figure 4 shows details of how the actuator and flap are attached together. Two cords connect the flap and actuator; each one is used to actuate the flap in opposing directions.

The electromechanical actuator is bolted to four aluminum brackets that are adhesively bonded to the main rotor blade spar. The bolted connections allow the actuator to be easily removed for

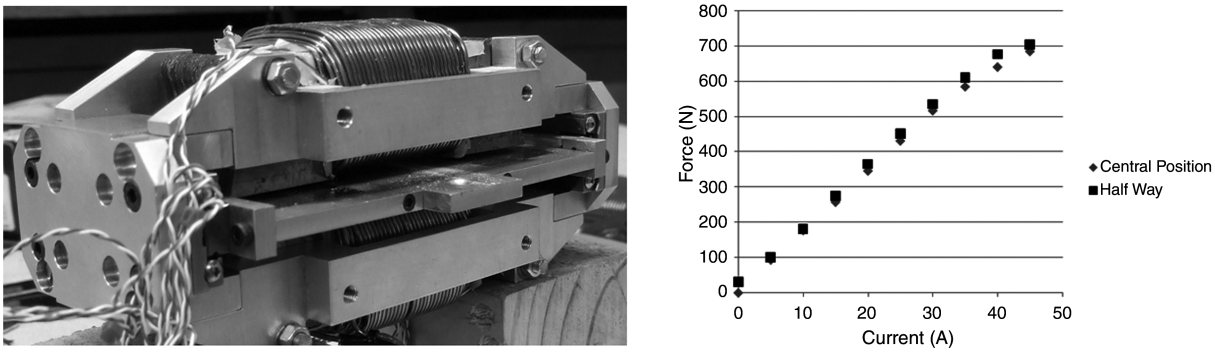

a) **b)**

Fig. 3 Actuator design and performance.

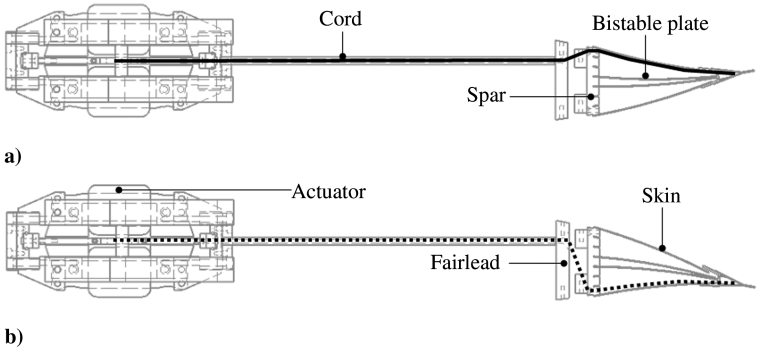

Fig. 4 Profile view of actuator and flap when a) flap is at 0 deg and b) flap is at 10 deg. The cord in tension is highlighted.

maintenance or replacement. The total mass of these brackets is approximately 2.0 kg. In total, the mass increase for installing the 1-m-span flap system into the rotor blade is approximately 6.3 kg. Less than one-half, 2.5 kg, of this mass is due to the actuator active parts. A mass of 3.0 kg is associated with the actuator housing and the actuator supporting structure in the D-spar, and the remaining 0.8 kg is associated with the trailing-edge mounted flap.

IV. Wind-Tunnel Testing

Wind-tunnel testing was required to quantify the effects on lift, drag, and pitching moment of deploying the bistable flap. These quantities are measured using an OR6-7 2000 series force platform manufactured by Advance Mechanical Technology, Inc., which is interfaced to a PC data logger using a DSpace unit. This force platform is attached to the rotor blade using two large struts passing though the aerodynamic center and one smaller central-sting attachment near the trailing edge (see Fig. 5a). These struts allow the blade to pitch ± 20 deg. To ensure two-dimensional flow, the gap between the ends of the rotor blade and the side walls of the wind tunnel was restricted to 10 mm (less than 0.5% of the full span of the tunnel). The actuator power supply is fed out of the side wall of the wind tunnel. The current and voltage supplied to the actuator were recorded in order to estimate the required electrical energy to change between geometries. It was found that a supply of 26 V providing a current of 45 A was sufficient to actuate the flap. During the tests this power was supplied for approximately 1 s to ensure snap-through, although, as indicated later, the actual transition occurred over a much shorter interval. The two stable geometries of the bistable airfoil are shown in Fig. 5b.

The University of Bristol's largest closed-section closed-circuit wind tunnel has an octagonal test section with dimensions of 7 ft (2.134 m) by 5 ft (1.524 m). For these tests, the angle of attack was varied between -16 and $+12$ deg in 2 deg increments at 60 m/s airspeed. For each of these increments, the flap was tested in both stable states and the force platform recorded the quasi-static values of lift coefficient C_l, drag coefficient C_d, and pitching moment coefficient C_m. After this, dynamic tests were undertaken to quantify the changes in these three coefficients as the flap transits between stable states while under aerodynamic loading. The polar plot results of a viscid XFOIL [16] model of the wind-tunnel demonstrator are shown in Fig. 6. The Reynolds number was taken to be 2.69×10^6. The 10 deg flap-deployed results were calculated using strip theory: a 1-m-span flap region combined with 1.114 m of standard NACA 24016 rotor blade section. The quasi-static experimental results are also plotted on Fig. 6. Two-dimensional tunnel boundary corrections have been included in the experimental results to account for wall effects [17]. The experimentally observed lift-curve slopes match the XFOIL predictions closely. The change in lift due to flap deployment is lower than predicted, however, and the experimentally observed drag coefficients are larger than predicted. The discrepancies in change in lift are likely to be due to the deformation of the manufactured flap under aerodynamic loading. The discrepancies in drag are mainly due to the effect of the strut supports as well as flap vortices emanating from the flap tips (not modeled in XFOIL) and surface imperfections. The detrimental effect of the supports becomes obvious when comparing the drag coefficient discrepancies between positive and negative angles of attack. For positive angles of attack, the supports are located on the suction surface of the blade, where they adversely affect the flow and possibly promote separation, at least over part of the span. On the other hand, for negative angles of attack, the supports are on the pressure surface, where the flow is more resistant to separation; thus, their adverse effect is constrained and the drag is not significantly increased. However, the results do show that the airfoil is not stalled for a wide range of angles of attack with the flap deployed and that the installation of the

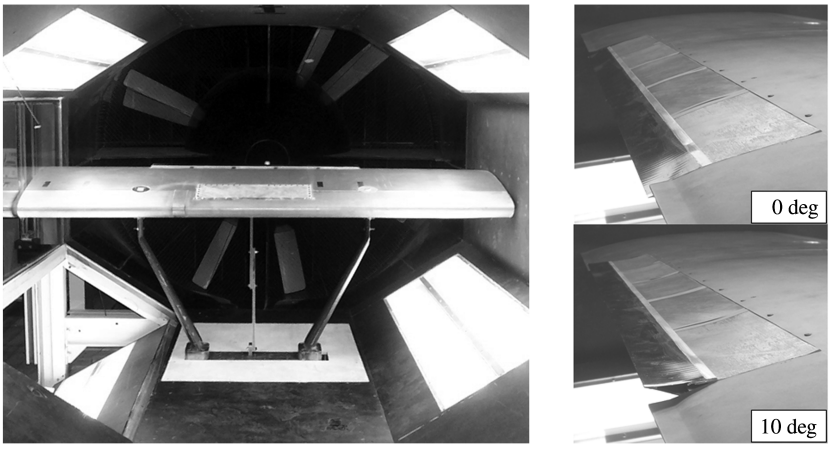

Fig. 5 Wind-tunnel demonstrator model: a) front view and b) stable flap states.

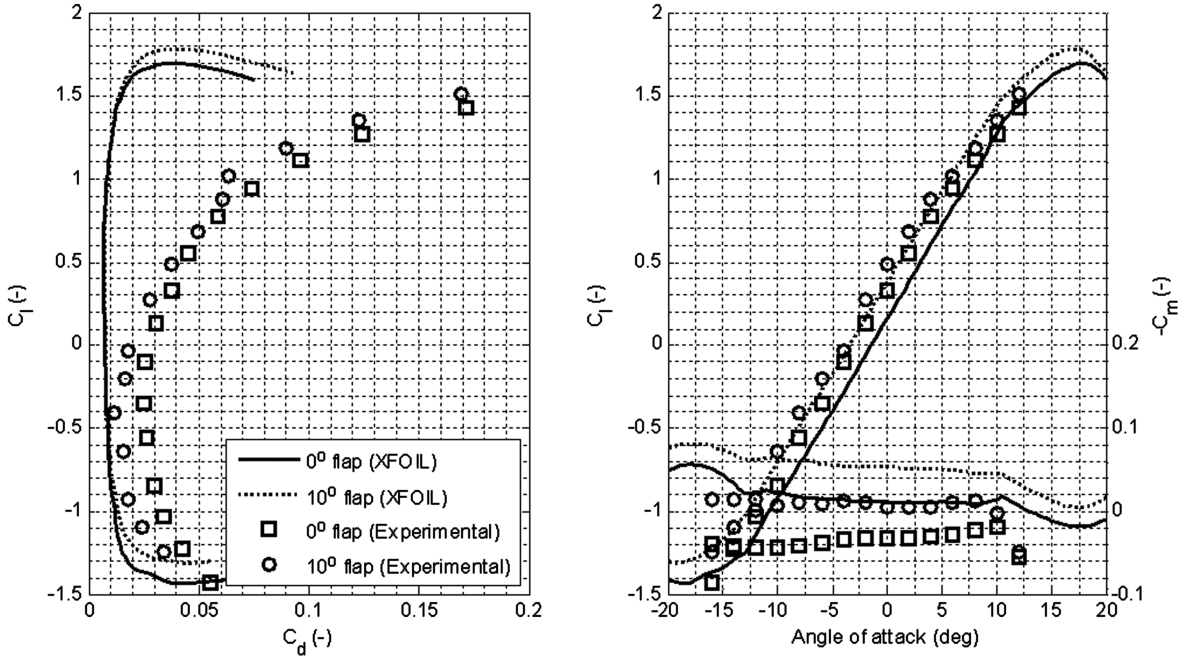

Fig. 6 Polar plot of IRCS bistable airfoil.

bistable flap does not initiate a premature stall. There were also no observed flutter instabilities for all of the wind-tunnel tests conducted. When the flap is deflected to 10 deg, there is an increase in lift coefficient of approximately 0.2.

The time-dependent variations of C_l, C_d, and C_m due to flap deployment are shown in Fig. 7. These plots were recorded at 60 m/s and 0 deg angle of attack for the flap moving from its 0 deg configuration to its 10 deg deployed configuration. The actuation voltage supplied was 26 V at 45 A over a time period of approximately 1 s. It can be seen that the snap-through event is nearly instantaneous and lasts no more than 0.05 s. The results show that there is effectively a step change in C_l and C_m. The coefficient of drag remains approximately constant over this transition period. It was found that the maximum workable frequency to actuate the flap continuously between flap states is limited by the overheating of the actuator.

V. Conclusions

The objectives of this wind-tunnel demonstrator model were to demonstrate the feasibility of using bistable composite materials for an active airfoil control surface and to evaluate the potential performance benefits. The use of bistable composites as aerodynamic surfaces was proven to be possible, and stable trailing-edge deflections of 0 and 10 deg were achieved. The wind-tunnel model clearly demonstrated a significant change in lift coefficients compared to the standard airfoil section when the flap was deflected. The mass increase for the integration of the actuated bistable flap system was approximately 6.3 kg per 1-m-span flap, with the active components of the actuator itself weighing 2.5 kg. This mass increase could potentially be reduced further with incremental design improvements and improved integration of the actuator parts within the blade structure. The flap system was able to actuate within 0.05 s in dynamic tests. The proposed flap design may also have dynamic

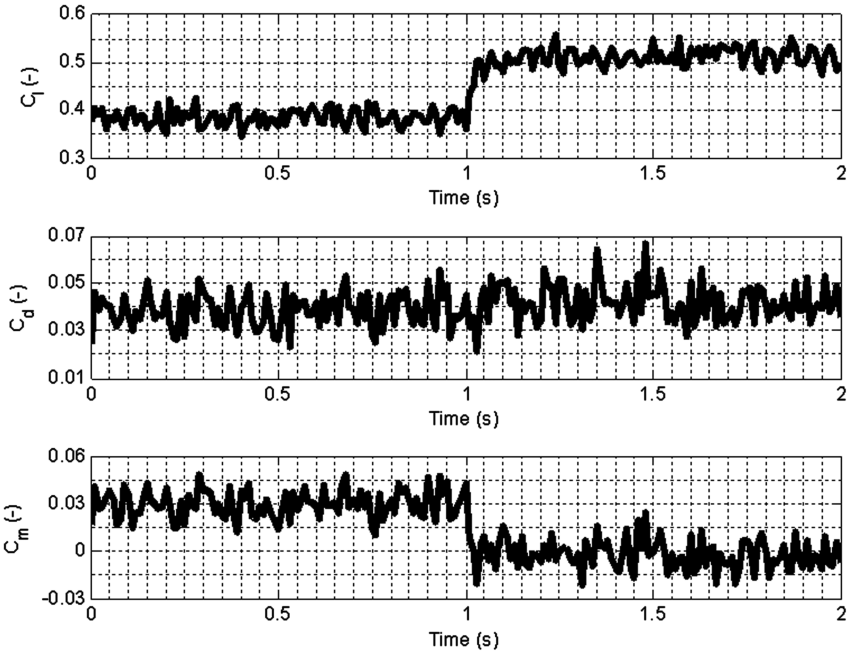

Fig. 7 Dynamic characteristics of flap deployment with 0 deg angle of attack.

applications for rotorcraft vibration/noise reduction that have yet to be explored. Follow-on whirl tower tests and more sophisticated simulations would be needed to fully quantify if there are any improvements in vibrations, noise, and aerodynamic performance over conventional mechanical flaps. These technologies may also have potential to be extended to nonhelicopter applications such as wind turbine blades.

Acknowledgments

Authors thank Simon Stacey at AgustaWestland for his assistance. The Intelligent Responsive Composite Structures (IRCS) project was partially funded by The U.K. Department for Business, Enterprise, and Regulatory Reform (BERR). IRCS industrial sponsors include AgustaWestland, GE Aviation, and Garrad-Hassan and Partners, Ltd.

References

[1] Campanile, L. F., and Anders, S., "Aerodynamic and Aeroelastic Amplification in Adaptive Belt-Rib Airfoils," *Aerospace Science and Technology*, Vol. 9, No. 1, Jan. 2005, pp. 55–63. doi:10.1016/j.ast.2004.07.007

[2] Straub, F. K., Kennedy, D. K., Stemple, A. D., Anand, V. R., and Birchette, T. S., "Development and Whirl Tower Test of the Smart Active Flap Rotor," *SPIE Industrial and Commercial Applications of Smart Structures Technologies*, International Society for Optical Engineering, Bellingham, WA, 16–18 Mar. 2004, pp. 202–212.

[3] Dieterich, O., Enenkl, B., and Roth, D., "Trailing Edge Flaps for Active Rotor Control Aeroelastic Characteristics of the ADASYS Rotor System," *American Helicopter Society 62nd Annual Forum*, AHS International, Alexandria, VA, 9–11 May 2006.

[4] Sanders, B., Cowan, D., and Scherer, L., "Aerodynamic Performance of the Smart Wing Control Effectors," *Journal of Intelligent Material Systems and Structures*, Vol. 15, No. 4, Apr. 2004, pp. 293–303. doi:10.1177/1045389X04042799

[5] Van Wingerden, J. W., Hulskamp, A. W., Barlas, T., Marrant, B., Van Kuik, G. A. M., Molenaar, D. P., and Verhaegen, M., "On the Proof of Concept of a 'Smart' Wind Turbine Rotor Blade for Load Alleviation," *Wind Energy Technology*, Vol. 11, No. 3, Jan. 2008, pp. 265–280. doi:10.1002/we.264

[6] Bak, C., Gaunaa, M., Andersen, P. B., Buhl, T., Hansen, P., Clemmensen, K., and Moeller, R., "Wind Tunnel Test on Wind Turbine Airfoil with Adaptive Trailing Edge Geometry," 45th AIAA Aerospace Sciences Meeting and Exhibit, Reno, NV, AIAA Paper 2007-10168–11 Jan. 2007.

[7] Buhl, T., Bak, D. C., Gaunaa, M., and Andersen, P. B., "Load Alleviation Through Adaptive Trailing Edge Control Surfaces: ADAPWING Overview," *European Wind Energy Conference and Exhibition*, European Wind Energy Association, Brussels, 7–10 May 2007, pp. 20–23.

[8] Hyer, M. W., "The Room-Temperature Shapes of Four Layer Unsymmetric Cross-Ply Laminates," *Journal of Composite Materials*, Vol. 16, No. 4, Mar. 1982, pp. 318–340. doi:10.1177/002199838201600406

[9] Potter, K. D., and Weaver, P. M., "A Concept for the Generation of Out-of-Plane Distortion from Tailored FRP Laminates," *Composites, Part A: Applied Science and Manufacturing*, Vol. 35, No. 12, Dec. 2004, pp. 1353–1361. doi:10.1016/j.compositesa.2004.06.022

[10] Daynes, S., Potter, K. D., and Weaver, P. M., "Bistable Prestressed Buckled Laminates," *Composites Science and Technology*, Vol. 68, Nos. 15–16, Oct. 2008, pp. 3431–3437. doi:10.1016/j.compscitech.2008.09.036

[11] Mattioni, F., Weaver, P. M., Friswell, M. I., and Potter, K. D., "Modelling and Applications of Thermally Induced Multistable Composites with Piecewise Variation of Layup in the Planform," 48th AIAA/ASME/ASCE/AHS/ASC Structures, Structural Dynamics, and Materials Conference, AIAA Paper 2007-2262, Honolulu, HI, 23–26 Apr. 2007.

[12] Diaconu, C. G., Weaver, P. M., and Mattioni, F., "Concepts for Morphing Airfoil Sections Using Bistable Laminated Composite Structures," *Thin-Walled Structures*, Vol. 46, No. 6, June 2008, pp. 689–701. doi:10.1016/j.tws.2007.11.002

[13] Daynes, S., Weaver, P. M., and Potter, K. D., "Aeroelastic Study of Bistable Composite Airfoils," *Journal of Aircraft*, Vol. 46, No. 6, 2009, pp. 2169–2174. doi:10.2514/1.44287

[14] Daynes, S., Weaver, P. M., Potter, K. D., and Hardick, M., U.K. Patent Application for a "Device Which is Subject to Fluid Flow," Docket No. 0902914.1, filed 20 Feb. 2009.

[15] Langley, F. L., and Mellor, P. H., "A Short-Stroke Permanent Magnet Aerospace Actuator with High Force-to-Mass Ratio," *IEEE Industrial Electronics, IECON 2006—32nd Annual Conference*, Inst. of Electrical and Electronics Engineers, Piscataway, NJ, 6–10 Nov. 2006, pp. 3199–3204.

[16] XFOIL, Software Package, Ver. 6.9, Massachusetts Inst. of Technology, Cambridge, MA, 2001.

[17] Barlow, J. B., Rae, H. R., and Pope, A., *Low-Speed Wind Tunnel Testing*, 3rd ed., Wiley, New York, 1999, pp. 349–363.